

Neutron diffraction and reverse Monte Carlo study of bulk amorphous $\text{Ga}_{38}\text{Sb}_{38}\text{Ge}_{24}$ alloys

A. I. Kolesnikov,^{1,*} O. I. Barkalov,¹ M. Calvo-Dahlborg,² U. Dahlborg,² W. S. Howells,³ and E. G. Ponyatovsky¹

¹*Institute of Solid State Physics, Russian Academy of Sciences, 142432 Chernogolovka, Moscow District, Russia*

²*LSG2M, CNRS UMR 7584, Ecole des Mines, Parc de Saurupt, 54042 Nancy Cedex, France*

³*ISIS Facility, Rutherford Appleton Laboratory, Chilton, Didcot, Oxon OX11 0QX, United Kingdom*

(Received 4 October 1999; revised manuscript received 29 March 2000)

The structure of bulk amorphous $\text{Ga}_{38}\text{Sb}_{38}\text{Ge}_{24}$ alloy produced by thermobaric treatment was studied at 100 K by neutron diffraction. The Fourier transformation of the measured structure factor clearly shows that two nearest-neighbor distances exist in the alloy. The results are compared to the ones obtained for the similarly produced amorphous GaSb, studied earlier. The analysis of the data reveals that the amorphous $\text{Ga}_{38}\text{Sb}_{38}\text{Ge}_{24}$ alloy is homogenous. The average nearest-neighbor coordination number obtained, 4.25, is greater than 4, indicating that the tetrahedral arrangements in the sample are distorted. Reverse Monte Carlo simulations were carried out using the measured structure factor of both alloys. It is shown that the degree of chemical disorder in both amorphous alloys is large.

I. INTRODUCTION

A process employing spontaneous amorphization of a quenched high-pressure phase in the course of heating from liquid nitrogen to ambient temperature at atmospheric pressure has recently been developed.¹ A series of bulk amorphous alloys were produced by this thermobaric method. The structure factor $S(Q)$ for some of them ($\text{Zn}_{41}\text{Sb}_{59}$, GaSb, and $\text{Al}_{32}\text{Ge}_{68}$) was determined by the neutron-diffraction (ND) technique.²⁻⁶ In the present work the structure of bulk amorphous $\text{Ga}_{38}\text{Sb}_{38}\text{Ge}_{24}$ alloy is investigated by ND and the results are analyzed using reverse Monte Carlo (RMC) simulations.^{7,8} RMC simulations have also been performed using the previously measured $S(Q)$ for the similarly produced amorphous GaSb alloy⁵ and the influence of Ge admixture on the structure of the sample will be discussed.

The pseudobinary GaSb-Ge system has a simple equilibrium phase diagram with eutectic and two phase equilibria in the solid state, GaSb+Ge. Quenching from the melt results in the formation of a metastable solid solution over the entire concentration region.⁹ The electrical resistivity of the solid solution produced has a typical semiconductor behavior. The long-range parameter of chemical ordering as a function of Ge concentration in the metastable solid solution decreases from 1 for pure GaSb to zero at 40 at. % Ge. From the variation of the electrical resistance in the T - P region it was supposed¹⁰ that a homogeneous metallic phase is formed at $P > 8-9$ GPa and $T > 400$ °C in the whole concentration range from pure GaSb to pure Ge. By x-ray examination of the quenched high-pressure phases it was shown¹¹ that a metallic phase with a β -Sn-type crystal structure was formed in GaSb-Ge alloys subjected to 7.0 GPa and 250 °C at Ge concentrations less than 30 at. % Ge. Thus, in order to have an initial single phase for the high-pressure crystalline state and a 100% amorphized sample after the solid-state amorphization, an alloy containing 24 at. % Ge was selected for further investigation.

II. EXPERIMENTAL DETAILS

To prepare the sample a crystalline powder of the GaSb-Ge alloy was first subjected to 7.7 GPa and 250 °C for

about 24 h. This was subsequently followed by cooling under pressure to liquid-nitrogen temperature and a release of the pressure to atmospheric. The final amorphous pellets in the form of discs, 7 mm in diameter and about 2 mm thick, were produced by slow heating at about 20 K/min to ~ 150 °C. After production, each tablet was checked for crystalline inclusions by x-ray diffraction and subsequently stored in a Dewar containing liquid nitrogen.

The ND experiment was carried out on the LAD diffractometer at the ISIS pulsed neutron source at the Rutherford Appleton Laboratory, UK.¹² The data were collected in a very wide range of neutron momentum transfer Q , from 0.5 to 35 \AA^{-1} . The ISIS pulsed neutron source produces neutrons with a spread of energies (or wavelengths) so that the intensity of neutrons scattered from the sample is measured at fixed angle detectors as a function of time-of-flight. The spectra obtained can be directly transformed to momentum transfer spectra. The time-of-flight technique makes it thus possible to measure a complete ND pattern over the entire momentum transfer range simultaneously.

The pellets of the $\text{Ga}_{38}\text{Sb}_{38}\text{Ge}_{24}$ alloy studied were packed into a cylindrical vanadium can of 8 mm inner diameter. The ND experiment was carried out at 100 K by using a standard helium cryostat. Measurements were done with the sample in the can, with the empty can and without the sample and can (the background measurement). The ND from an 8 mm diameter vanadium rod was also measured, for normalization purposes. The time-of-flight spectrum obtained was transformed to the structure factor $S(Q)$ by using the ATLAS correction program package.¹³ The pair distribution function $G(r)$ was then calculated by Fourier transformation of the $S(Q)$ spectrum (with $Q_{\text{max}} = 35 \text{ \AA}^{-1}$) using the standard transformation technique

$$G(r) = 1 + \frac{1}{2\pi^2\rho_0 r} \int_0^{Q_{\text{max}}} Q[S(Q) - 1] \times \sin(Qr) \frac{\sin \alpha(Q)}{\alpha(Q)} dQ, \quad (1)$$

TABLE I. The relative weights of different atomic pairs contributing to the total structure factor and the total radial distribution function for amorphous $\text{Ga}_{38}\text{Sb}_{38}\text{Ge}_{24}$ sample.

Ga-Ga	Ga-Ge	Ga-Sb	Ge-Ge	Ge-Sb	Sb-Sb
0.25	0.17	0.19	0.12	0.13	0.14

ρ_0 is the average atomic density ($0.03693 \text{ at./\AA}^3$ corresponding to $5.53 \pm 0.05 \text{ g/cm}^3$) and the modification function $\alpha(Q)$ is given by $\alpha(Q) = \pi Q / Q_{\text{max}}$.

III. DATA ANALYSIS AND RESULTS

The gallium, antimony, and germanium nuclei are predominantly coherent scatterers of neutrons. The corresponding scattering cross sections are $\sigma_{\text{Ga}}^{\text{coh}} = 6.675 \text{ barn}$, $\sigma_{\text{Sb}}^{\text{coh}} = 3.90 \text{ barn}$, and $\sigma_{\text{Ge}}^{\text{coh}} = 8.42 \text{ barn}$.¹⁴ Because the sample studied is a three-component system, it is essential to know the magnitude of the different structural correlations which contribute to the total scattering intensity. This is equivalent to estimating the contribution of the partial structure factors $S_{ij}(Q)$ to the total $S(Q)$ and the partial atom-atom pair distribution functions to $G(r)$. These contributions are given by the following expression:

$$S(Q) = \sum_{ij} \sqrt{x_i x_j \sigma_i^{\text{coh}} \sigma_j^{\text{coh}}} S_{ij}(Q), \quad (2)$$

where the sum is over all the different types of atomic pairs (i, j), x_i being the concentration of atom of type i . The partial structure factor $S_{ij}(Q)$ is related to the partial atom-atom pair distribution function $G_{ij}(r)$ by¹⁵

$$S_{ij}(Q) = \delta_{ij} + 4\pi\rho_0 \sqrt{x_i x_j} \int_0^\infty [G_{ij}(r) - 1] \frac{\sin(Qr)}{Qr} r^2 dr. \quad (3)$$

The relative weights of the oscillating part of the partial structure factors are given in Table I. From Table I it can be seen that all the different atom-atom correlations contribute to the total functions; none is negligible. Figures 1 and 2(a) show the experimentally obtained structure factor $S(Q)$ and

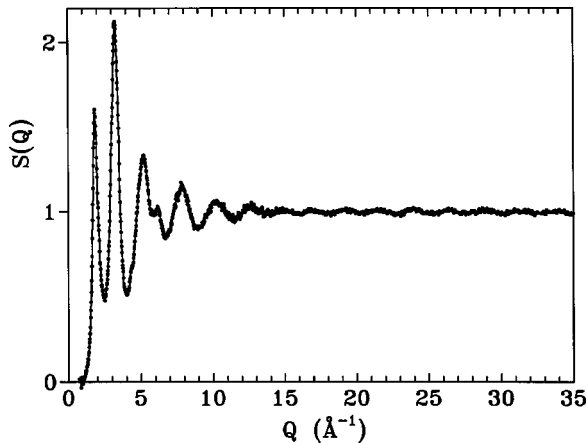


FIG. 1. The structure factor $S(Q)$ for amorphous $\text{Ga}_{38}\text{Sb}_{38}\text{Ge}_{24}$ at 100 K.

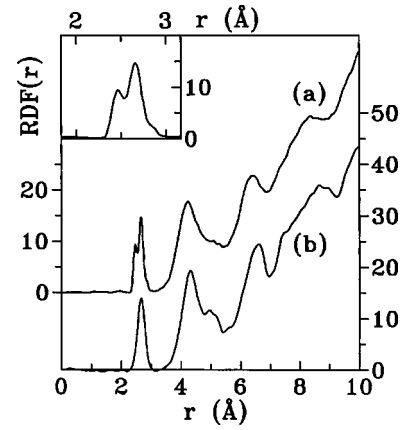


FIG. 2. The total radial distribution function, $\text{RDF}(r) = 4\pi r^2 \rho_0 G(r)$, for amorphous (a) $\text{Ga}_{38}\text{Sb}_{38}\text{Ge}_{24}$ and (b) GaSb (Ref. 5) alloys at 100 K. The inset shows the $\text{RDF}(r)$ around the first peak for $\text{Ga}_{38}\text{Sb}_{38}\text{Ge}_{24}$ in a larger r scale.

the total radial distribution function calculated from the expression $\text{RDF}(r) = 4\pi r^2 \rho_0 G(r)$ for the amorphous $\text{Ga}_{38}\text{Sb}_{38}\text{Ge}_{24}$. The experimental data clearly show that the sample studied is a good quality amorphous material. No diffraction peaks, characteristic of crystalline inclusions, are observed in the ND patterns even at large scattering angles (where the resolution $\Delta Q/Q = 0.6\%$). There was a possibility that the $\text{Ga}_{38}\text{Sb}_{38}\text{Ge}_{24}$ sample was not a homogeneous amorphous material and that it might consist of a mixture of two kinds of clusters, amorphous GaSb and amorphous Ge. This possibility was checked by small-angle neutron-scattering on an amorphous sample of the same composition as the present one.¹⁶ No strong signal was recorded which would have been the case if the sample had been consisting of two components, GaSb and Ge, (the amorphous Ge has higher coherent neutron scattering per unit volume compared to the average value for $\text{Ga}_{38}\text{Sb}_{38}\text{Ge}_{24}$). Thus, from the small-angle neutron scattering and the ND data it can be concluded that the $\text{Ga}_{38}\text{Sb}_{38}\text{Ge}_{24}$ sample studied is not only amorphous but also homogeneous.

The comparison of the present $S(Q)$ data for $\text{Ga}_{38}\text{Sb}_{38}\text{Ge}_{24}$ with that for the similarly produced amorphous GaSb (Ref. 5) and pure amorphous Ge produced by the deposition technique¹⁷ shows that the spectra are very similar in shape, which indicates that the three amorphous materials have a similar structure, of the tetrahedral type. However, the peak positions are different. The number density of the amorphous $\text{Ga}_{38}\text{Sb}_{38}\text{Ge}_{24}$ ($\rho_0 = 0.03693 \text{ at./\AA}^3$) is between the values for Ge ($\rho_0 = 0.03975 \text{ at./\AA}^3$) and GaSb ($\rho_0 = 0.0343 \text{ at./\AA}^3$). The difference in sample density itself is reflected in the different positions for the peaks in the structure factor $S(Q)$; they are shifted to higher Q for larger sample densities. Table II gives the position and the full width at half maximum (FWHM) as determined for the first two peaks of $S(Q)$ for Ge, GaSb, and $\text{Ga}_{38}\text{Sb}_{38}\text{Ge}_{24}$. The values of FWHM of the first two peaks are related to the correlation lengths in the amorphous sample by the expressions $\chi_{CC} = 2\pi/\Delta Q_1$ and $\chi_{NN} = 2\pi/\Delta Q_2$ for the chemical and density fluctuations, respectively. For the $\text{Ga}_{38}\text{Sb}_{38}\text{Ge}_{24}$ alloy the correlation lengths are found to be similar to those for amorphous Ge, $\chi_{CC} = 15 \text{ \AA}$ and $\chi_{NN} = 11 \text{ \AA}$, compared with $\chi_{CC} = 19 \text{ \AA}$ and $\chi_{NN} = 10 \text{ \AA}$ for amorphous GaSb. This

TABLE II. Parameters obtained from a Gaussian fit of the first two peaks of $S(Q)$ for amorphous Ge (Ref. 17), GaSb (Ref. 5), and $\text{Ga}_{38}\text{Sb}_{38}\text{Ge}_{24}$. All values are in \AA^{-1} .

Sample	The first peak		The second peak	
	Position	FWHM	Position	FWHM
Ge	1.88	0.43	3.38	0.56
GaSb	1.80	0.33	3.14	0.60
$\text{Ga}_{38}\text{Sb}_{38}\text{Ge}_{24}$	1.86	0.42	3.24	0.56

indicates that the chemical order in $\text{Ga}_{38}\text{Sb}_{38}\text{Ge}_{24}$ is slightly lower than in amorphous GaSb (due to admixture of Ge), but the density fluctuations are about the same. The difference in the position of the second (the so-called ‘‘principal’’) peak for the three compounds and their similar widths support the above conclusion, that the $\text{Ga}_{38}\text{Sb}_{38}\text{Ge}_{24}$ sample is homogeneous. In the case of a mixture of two amorphous alloys, GaSb and Ge, the FWHM of the second peak in $S(Q)$ would be much larger or even split.

The RDF(r) function for amorphous $\text{Ga}_{38}\text{Sb}_{38}\text{Ge}_{24}$, shown in Fig. 2(a), is very different from that obtained for bulk amorphous GaSb [see Fig. 2(b)] in that it exhibits a very distinct split of the first peak. The positions of the two maxima are at 2.46 and 2.66 \AA . The splitting of the first peak reflects the existence of two different nearest-neighbor correlations. For quantitative purposes the first peak was fitted by a sum of three Gaussian functions and the results are listed in Table III. The covalent radii r^{cov} for Ga, Sb, and Ge, atoms are equal to 1.26, 1.38, and 1.22 \AA , respectively. The first maximum in RDF(r) ($r=2.46 \text{\AA}$) is close to $2r_{\text{Ge}}^{\text{cov}}$ and to $r_{\text{Ge}}^{\text{cov}}+r_{\text{Ga}}^{\text{cov}}$, and is thus obviously related to Ge-Ge and Ge-Ga correlations. The second maximum at $r=2.66 \text{\AA}$ corresponds to $r_{\text{Ga}}^{\text{cov}}+r_{\text{Sb}}^{\text{cov}}$ and $r_{\text{Ge}}^{\text{cov}}+r_{\text{Sb}}^{\text{cov}}$ and may thus be assigned to Ga-Sb and Ge-Sb correlations. The shoulder observed on the right-hand side (the third Gaussian peak, see Table III) at 2.86 \AA reveals the presence of Sb-Sb pairs. The Ga-Ga pair correlations, with $2r_{\text{Ga}}^{\text{cov}}=2.52 \text{\AA}$, if they exist, are probably more spread over longer distances and may thus give contributions in between the above mentioned two maxima. It follows from Table III that the total average coordination number for the nearest neighbors in amorphous $\text{Ga}_{38}\text{Sb}_{38}\text{Ge}_{24}$ is 4.25, which indicates that the atomic arrangement in this alloy deviates from that of a regular tetrahedral network. However, the ratio between the position of the second peak (at $\sim 4.19 \text{\AA}$) in RDF(r) and the average position for the first one ($\sim 2.59 \text{\AA}$) is close to the ideal tetrahedral value, 1.633.

TABLE III. Parameters obtained from a fit of the first peak of the RDF(r) for $\text{Ga}_{38}\text{Sb}_{38}\text{Ge}_{24}$ by a sum of three Gaussian functions.

Gaussian number	Position of peak (\AA)	Width of peak (\AA)	Average coordination number
1	2.46	0.14	1.36
2	2.66	0.17	2.66
3	2.86	0.11	0.23

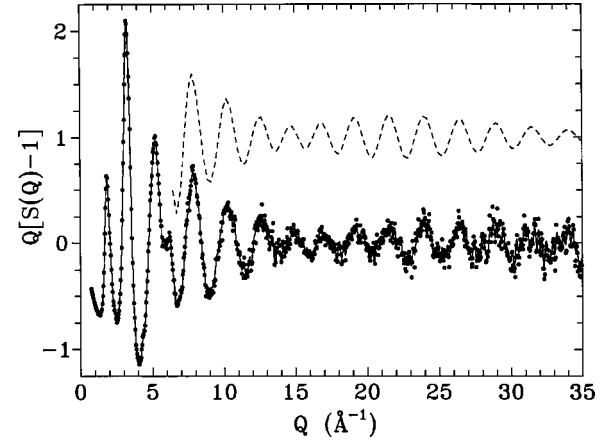


FIG. 3. The experimental reduced structure factor $Q[S(Q)-1]$ (points) and the RMC fit (solid line) for amorphous $\text{Ga}_{38}\text{Sb}_{38}\text{Ge}_{24}$. Vertically shifted short dashed line shows the reduced structure factor simulated at large Q values by using Eq. (4).

IV. REVERSE MONTE CARLO SIMULATION

Because the neutron-scattering cross sections for different atoms in the alloy studied are different (see Sec. III above), it is in principle possible to get more information on the partial atomic correlations by analyzing the experimental data with the RMC technique.^{7,8} In this computer model, a box is filled with atoms and, using the usual periodic boundary conditions, the pair-distribution function $G(r)$ and the structure factor $S(Q)$ are calculated for the particular atomic configuration. The atoms are then allowed to move until the calculated $S(Q)$ agrees with the experimental data within the experimental errors. The final atomic configuration is stored as a three-dimensional structure which can be used for physical estimates of the structure of the real system.

RMC calculations were made for $\text{Ga}_{38}\text{Sb}_{38}\text{Ge}_{24}$ and GaSb alloys in a cubic box of size 60.058 and 61.556 \AA , respectively, containing in total 8000 atoms, randomly distributed with an atomic composition according to the actual chemical composition and density. The calculated $S(Q)$ for both

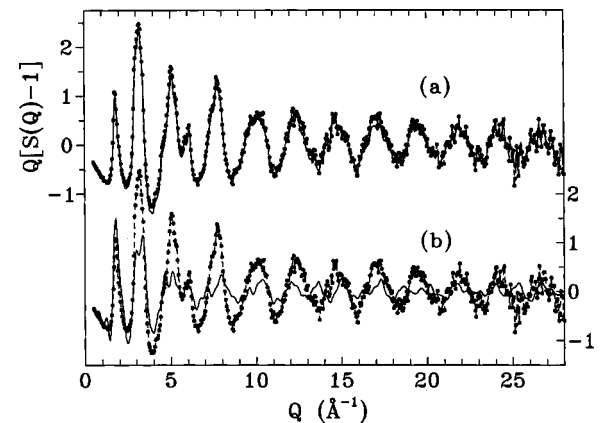


FIG. 4. The experimental reduced structure factor $Q[S(Q)-1]$ (dashed line with points) and the RMC fit (solid line) for amorphous GaSb with (a) no constraints on the chemical order in the alloy, and (b) with constraints, allowing only 10% of the nearest neighbors to be the atoms of the same type (see the text). The left and the right y axis are for (a) and (b) curves, respectively.

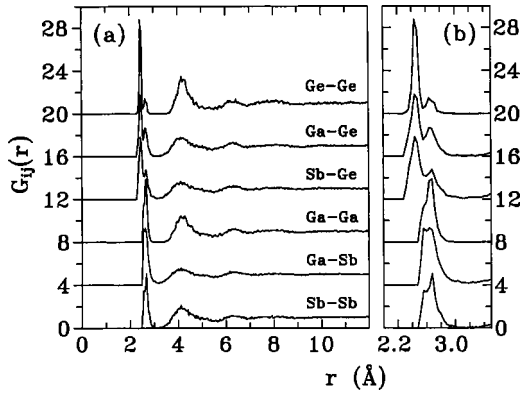


FIG. 5. Partial radial distribution functions $G_{ij}(r)$ for amorphous $\text{Ga}_{38}\text{Sb}_{38}\text{Ge}_{24}$ obtained by RMC modeling plotted in a whole simulated area (a), and in a larger r scale for the first peak only (b).

samples fit the experimental data very well as shown in Figs. 3 and 4 (top curve). The partial radial distribution functions $G_{ij}(r)$ obtained are plotted in Figs. 5 and 6. The atomic correlations were analyzed using the three-dimensional atomic coordinates, and the average partial coordination numbers n_{ij} obtained from the results of the RMC simulations for the different atomic pairs are presented in Table IV. The distributions of atom-atom nearest neighbors are shown in Figs. 7 and 8 for amorphous $\text{Ga}_{38}\text{Sb}_{38}\text{Ge}_{24}$ and GaSb alloys, respectively.

The RMC results for amorphous GaSb (Fig. 6) show the existence of a large amount of nearest-neighbor pairs of the same kind of atoms, with a rather narrow distance distribution [the first peaks in $G_{ij}(r)$ functions for Ga-Ga and Sb-Sb]. Their contributions to the second peak in $G(r)$ are definitely the dominating ones. The intensity under the second peak for Ga-Sb correlations is small but not negligible (see Fig. 6) as should be the case for a tetrahedrally coordinated network with ideal chemical order. As for the results of RMC simulations for $\text{Ga}_{38}\text{Sb}_{38}\text{Ge}_{24}$ (Fig. 5), the first peaks in the partial $G_{ij}(r)$ s exhibit a complicated behavior. They have two main maxima, one at smaller distance for Ge-containing pairs, and another one for other pairs. The positions of the maxima correspond to the values for two maxima in the radial distribution function obtained by Fourier transformation of the experimental structure factor. The Ga-Sb, Ga-Ga, and Sb-Sb correlations are similar to those obtained in RMC simulations for amorphous GaSb, but with broader distributions for pair correlations of atoms of the same type.

The existence of two nearest-neighbor correlations for the

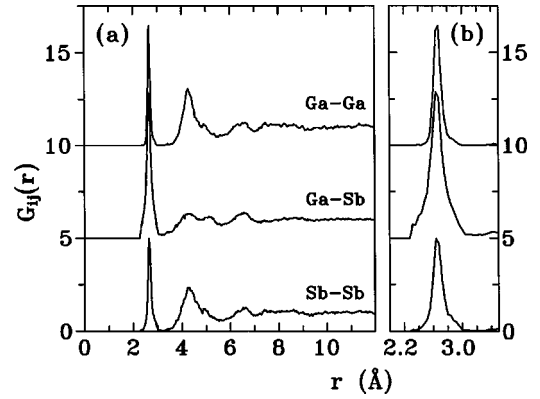


FIG. 6. The same as in the Fig. 5, for GaSb.

sample studied results in an interesting behavior of the structure factor at large neutron momentum transfers. It is clearly seen in Fig. 3 that the reduced structure factor $Q[S(Q) - 1]$ oscillates around zero, but while the amplitude of the oscillations gradually decreases for the GaSb sample [see Fig. 4(a)], at first it decreases with Q (up to 15 \AA^{-1}), then increases with a maximum around $23\text{--}24 \text{ \AA}^{-1}$, and finally decreases again at higher Q for $\text{Ga}_{38}\text{Sb}_{38}\text{Ge}_{24}$. The similar modulation was recently observed in the structure factor for vitreous P_2O_5 (Ref. 17). This behavior can be understood by assuming that at high Q values the main contributions to $S(Q)$ are determined by the short-range orders. To interpret qualitatively this modulation the following approximation was used for the reduced structure factor at high momentum transfers¹⁸

$$Q[S(Q) - 1] = \sum_i n_i \frac{\sin(Qr_i)}{Qr_i} \exp(-Q^2 \sigma_i^2). \quad (4)$$

Here r_i represents the first and the second nearest atom-atom distances, and n_i and σ_i are the coordination number and the spread of the corresponding atom-atom distribution, respectively. The vertically shifted dashed line in Fig. 3 shows the fit to the experimental data by the above expression, where two first-nearest-neighbor distances, $r_{11} = 2.46 \text{ \AA}$ and $r_{12} = 2.66 \text{ \AA}$, and the value of $r_2 = 4.19 \text{ \AA}$ were used, in accordance with the discussion on RDF(r) above, and n_i and σ_i being adjustable parameters. It is clear from Fig. 3, that the modulation observed in the spectrum for $\text{Ga}_{38}\text{Sb}_{38}\text{Ge}_{24}$ is due to the difference in the periods of the corresponding oscillations which, of course, in turn is due to the different r_{11} and r_{12} values.

TABLE IV. The partial average coordination numbers n_{ij} for different atomic pairs obtained from the results of RMC simulations for GaSb and $\text{Ga}_{38}\text{Sb}_{38}\text{Ge}_{24}$ amorphous alloys.

Sample	Partial average coordination number, n_{ij}			$\sum_j n_{ij}$
$\text{Ga}_{38}\text{Sb}_{38}\text{Ge}_{24}$	$n_{\text{GaGa}} = 1.30$	$n_{\text{GaSb}} = 1.80$	$n_{\text{GaGe}} = 1.01$	$n_{\text{Ga}} = 4.11$
	$n_{\text{SbGa}} = 1.80$	$n_{\text{SbSb}} = 1.26$	$n_{\text{SbGe}} = 1.14$	$n_{\text{Sb}} = 4.20$
	$n_{\text{GeGa}} = 1.60$	$n_{\text{GeSb}} = 1.80$	$n_{\text{GeGe}} = 0.75$	$n_{\text{Ge}} = 4.15$
GaSb	$n_{\text{GaGa}} = 1.40$	$n_{\text{GaSb}} = 2.98$		$n_{\text{Ga}} = 4.38$
	$n_{\text{SbGa}} = 2.98$	$n_{\text{SbSb}} = 1.48$		$n_{\text{Sb}} = 4.46$

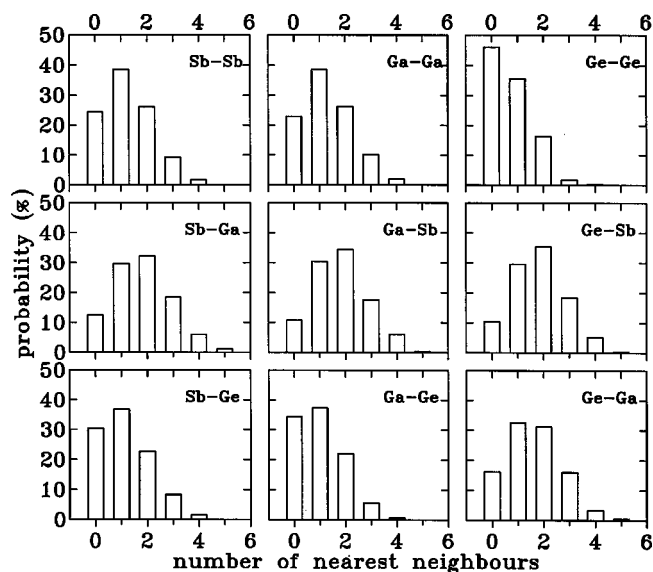


FIG. 7. The distribution of the number of neighbors n_{ij} within the first coordination shell for different atomic pairs in amorphous $\text{Ga}_{38}\text{Sb}_{38}\text{Ge}_{24}$ obtained from the RMC simulations.

It follows from Table IV and Fig. 7 that the Ge atoms do not construct a significant amount of amorphous clusters of tetrahedrally coordinated network because the average Ge-Ge coordination number, 0.75, is much smaller than 4, which is required for this situation. Actually, the value for n_{GeGe} is the smallest, which is easy to understand if one assumes a random distribution of Ge atoms and takes the low Ge concentration in the sample into account. Thus, it can be concluded that in the amorphous alloy studied the Ge atoms randomly substitute the Ga and Sb atoms in the corresponding GaSb alloy, but in doing so the nearest-neighbor distances between Ge and Ga/Sb atoms are modified in order to be closer to the value corresponding to the sum of their covalent radii. Note that the intensity of the second peak in the RMC simulated partial $G_{ij}(r)$ for Ge-Ge is higher compared to others (see Fig. 5), indicating some kind of ordering of Ge atoms on the apexes of tetrahedral units.

The partial $G_{ij}(r)$ curves for both GaSb and $\text{Ga}_{38}\text{Sb}_{38}\text{Ge}_{24}$ show rather large chemical disorder. The nearest neighbors are expected to be the atoms predominantly of different kind, especially in the case of GaSb. The degree of chemical disorder in an amorphous GaSb alloy, produced by solid-state amorphization, was analyzed by extended x-ray-absorption fine-structure (EXAFS) measurements.¹⁹ The average number of nearest neighbors (at 78 K) in the first shell of the Ga-Ga pairs was found to be 0.7 ± 0.5 , while it was close to zero for crystalline GaSb sample. The correlations of Sb-Sb pairs in the amorphous sample were found to be negligibly small. The errors in the determination of the average nearest-neighbor numbers were relatively large (e.g., ranging from 0.5 to 0.7–0.8 for Ga-Ga). The chemical disorder in amorphous GaSb was furthermore analyzed from the distortion of the shape the first peak in a Fourier transform of the EXAFS signal and from temperature variation of the Debye-Waller broadening, compared to that of a crystalline sample.¹⁹ The authors¹⁹ concluded that the degree of chemical disorder in the material is below the accuracy of the EXAFS technique. Contrary to these results, the present

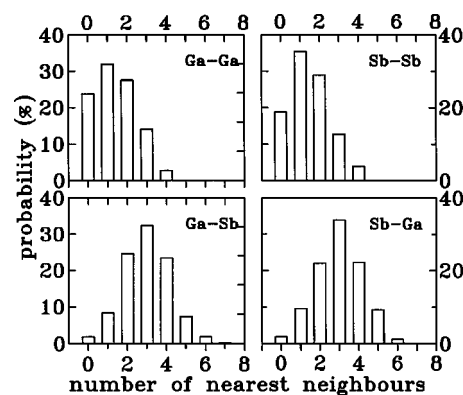


FIG. 8. The same as in the Fig. 7, for amorphous GaSb.

RMC simulations (see Table IV) show that the values for the average nearest-neighbor correlations for the atoms of the same type, Ga-Ga and Sb-Sb pairs, in both amorphous alloys, GaSb and $\text{Ga}_{38}\text{Sb}_{38}\text{Ge}_{24}$, are rather large (about 30%). Note, that the crystalline analog of bulk amorphous GaSb, GaSb-I, has a completely chemically ordered structure, with the nearest-neighbor pairs constructed exclusively from different atoms, Ga and Sb.

It should be noted that the RMC modeling is a mathematical method to derive a structure describing the measured $S(Q)$ and no special restrictions are imposed (especially energy minimization). When using RMC, one can get several different atomic structures that fit the experimental $S(Q)$ spectrum equally well, but generally one arrives at the most disordered one. In order to check for any other possible spatial arrangement of atoms in amorphous GaSb, further RMC simulations were made. They were started from an ordered structure, corresponding to the crystal structure for GaSb-I, and included constraints restricting the existence of nearest neighbors of the same type of atoms at distances smaller than 3 Å (i.e., in the first coordination shell). It was impossible to fit the experimental data with these constraints. Changing the constraints to allow 10% of the atoms of the same kind to be nearest neighbors, did not improve the quality of the fit. The example of one of the “best” fits with this kind of constraints is shown in Fig. 4(b). These calculations strongly support the RMC results obtained: that a large chemical disorder exists in both bulk amorphous $\text{Ga}_{38}\text{Sb}_{38}\text{Ge}_{24}$ and GaSb alloys.

To understand this very large chemical disorder in the amorphous alloys it is worth while to remember that both $\text{Ga}_{38}\text{Sb}_{38}\text{Ge}_{24}$ and GaSb were produced by solid-state amorphization in the course of slow heating of the quenched high-pressure phases. The high-pressure GaSb-II phase has been described as having a disordered β -tin structure^{20–22} and as well as having a disordered orthorhombic structure with a space group *Imma*.²³ This difference in the structural interpretation of the GaSb-II phase is discussed in Ref. 5, but here it should only be emphasized that all results indicate a very large degree of chemical disorder in the high-pressure phase. The amorphization process which takes place on heating to 150 °C probably involves changes mainly in the local arrangements of atoms without any long distance displacement which is required to create chemical order in the sample.

V. CONCLUSIONS

From the discussion above the following conclusions can be made:

(a) The $\text{Ga}_{38}\text{Sb}_{38}\text{Ge}_{24}$ alloy produced by solid-state amorphization of the quenched high-pressure phase can be regarded as a homogenous bulk amorphous compound.

(b) The short-range order in the amorphous $\text{Ga}_{38}\text{Sb}_{38}\text{Ge}_{24}$ alloy is different from that for amorphous GaSb. The average nearest-neighbor atomic coordination number obtained, 4.25, is greater than 4, indicating a distortion of an ideal tetrahedral arrangement in the alloy. Furthermore, there are two rather well defined nearest-neighbor distances.

(c) The analyses of the results of the RMC simulations show a random distribution of Ge atoms in amorphous $\text{Ga}_{38}\text{Sb}_{38}\text{Ge}_{24}$ alloy. The Ge atoms do not form any clusters with tetrahedrally coordinated arrangements, but randomly substitute the Ga and Sb atoms as compared to amorphous GaSb. Some degree of ordering of Ge atoms on the apexes of

tetrahedral units in $\text{Ga}_{38}\text{Sb}_{38}\text{Ge}_{24}$ can nevertheless be anticipated from the analyses of the RMC simulated partial $G(r)$ functions.

(d) According to the results of RMC simulations a large chemical disorder was found to exist in amorphous $\text{Ga}_{38}\text{Sb}_{38}\text{Ge}_{24}$ and GaSb alloys. About 30% of the nearest neighbors in the alloys are formed from atoms of the same kind (Ga-Ga and Sb-Sb pairs).

ACKNOWLEDGMENTS

This work has partly been financed by the CNRS—Russian Academy of Science Collaboration Agreement under Contract No. 4069, by the Royal Swedish Academy under Contract No. 1454, by the RFBR Grants No. 96-15-96806 and No. 99-02-17007. The authors would also like to thank ISIS for the provision of neutron beam facilities. O.I.B thanks the Alexander von Humboldt Foundation for financial support.

*Corresponding author. Present address: Department of Physics, UMIST, P.O. Box 88, Manchester M60 1QD, UK.

¹E. G. Ponyatovsky and O. I. Barkalov, *Mater. Sci. Eng., A* **133**, 726 (1991).

²O. I. Barkalov, A. I. Kolesnikov, E. G. Ponyatovsky, U. Dahlborg, R. Delaplane, and A. Wannberg, *J. Non-Cryst. Solids* **176**, 263 (1994).

³O. I. Barkalov, A. I. Kolesnikov, V. E. Antonov, E. G. Ponyatovsky, U. Dahlborg, M. Dahlborg, and A. C. Hannon, *Phys. Status Solidi B* **198**, 491 (1996).

⁴U. Dahlborg, M. Calvo-Dahlborg, A. I. Kolesnikov, O. I. Barkalov, V. E. Antonov, and E. G. Ponyatovsky, *Mater. Sci. Eng., A* **226**, 448 (1997).

⁵M. Calvo-Dahlborg, U. Dahlborg, A. I. Kolesnikov, O. I. Barkalov, E. G. Ponyatovsky, and A. C. Hannon, *J. Non-Cryst. Solids* **244**, 250 (1999).

⁶A. I. Kolesnikov, U. Dahlborg, M. Calvo-Dahlborg, O. I. Barkalov, E. G. Ponyatovsky, W. S. Howells, and A. I. Harkunov, *Phys. Rev. B* **60**, 12 681 (1999).

⁷R. L. McGreevy and L. Pustai, *Mol. Simul.* **1**, 359 (1988).

⁸D. A. Keen and R. L. McGreevy, *Nature (London)* **344**, 423 (1990).

⁹K. N. Ishihara, P. H. Shingu, H. Matsueda, and Y. Furuhashi, *Trans. Jpn. Inst. Met., Suppl.* **29**, 249 (1988).

¹⁰V. V. Brazhkin, A. G. Lyapin, S. V. Popova, and N. V. Kalyaeva, *J. Mater. Sci.* **30**, 443 (1995).

¹¹V. E. Antonov, O. I. Barkalov, E. G. Ponyatovsky, and Z. A. Zavolovich, *High Press. Res.* **15**, 201 (1997).

¹²*ISIS Experimental Facilities*, edited by B. Boland and S. Whapham (Rutherford Appleton Laboratory, UK, 1992).

¹³A. K. Soper, W. S. Howells, and A. C. Hannon, *ATLAS Analysis of Time-of-Flight Diffraction Data From Liquid and Amorphous Samples* (Rutherford Appleton Laboratory, UK, 1989).

¹⁴V. F. Sears, *Neutron News* **3**, 29 (1992).

¹⁵N. W. Ashcroft and D. C. Langreth, *Phys. Rev.* **159**, 500 (1967).

¹⁶M. Calvo-Dahlborg, U. Dahlborg, A. I. Kolesnikov, O. I. Barkalov, E. G. Ponyatovsky, and D. Lairez (unpublished).

¹⁷U. Hoppe, G. Walter, A. Barz, D. Stachel, and A. C. Hannon, *J. Phys.: Condens. Matter* **10**, 261 (1998).

¹⁸G. Etherington, A. C. Wright, J. T. Wenzel, J. C. Dore, J. H. Clarke, and R. N. Sinclair, *J. Non-Cryst. Solids* **48**, 265 (1982).

¹⁹A. V. Sapelkin, S. C. Bayliss, A. G. Lyapin, V. V. Brazhkin, and A. J. Dent, *Phys. Rev. B* **56**, 11531 (1997).

²⁰S. T. Weir, Y. K. Vohra, and L. A. Ruoff, *Phys. Rev. B* **36**, 4543 (1987).

²¹V. F. Degtyareva, I. T. Belash, E. G. Ponyatovsky, and V. I. Rashupkin, *Fiz. Tverd. Tela (Leningrad)* **32**, 1429 (1990) [*Sov. Phys. Solid State* **32**, 834 (1990)].

²²A. San Miguel, A. Polian, and J. P. Itié, *High Press. Res.* **10**, 416 (1992).

²³M. I. McMahon, R. J. Nelmes, N. G. Wright, and D. R. Allen, *Phys. Rev. B* **50**, 13 047 (1994).